Microchannels Analogues for the Study of Viscoelastic Fluid Flows Through Porous Media

Francisco J. GALINDO-ROSALES [1,*], Laura CAMPO-DEAÑO [2], Mónica S.N. OLIVEIRA [1], Manuel A. ALVES [1], Fernando T. PINHO [2], Evelien v. BOKHORST [1, 3], Peter J. HAMERSMA [3]

* Corresponding author: Tel.: +351 225 081 079; Fax: ++351 225 081 440; Email: galindo@fe.up.pt
1: Transport Phenomena Research Centre, Dept. Chemical Engineering, University of Porto, Portugal
2: Transport Phenomena Research Centre, Dept. Mechanical Engineering, University of Porto, Portugal
3: Dept. Chemical Engineering, University of Delft, The Netherlands

Abstract This work studies the flow behavior and related pressure losses of viscoelastic polymer solutions in microchannels with two different sequences of contraction/expansion, disposed in a symmetric and an asymmetric arrangement, respectively. These microfluidic devices are proposed as simplified microchannel analogues for the flow of Newtonian and viscoelastic fluids through porous media. The results show that the symmetric configuration mimics the pressure gradient of these polymer solutions through a porous medium at low flow rates (below a critical Deborah number, De_{cr}), while the asymmetric arrangement gives the asymptotic limit at high *De* values (above De_{cr}) as a consequence of the intrinsic differences in the extensional rate profiles defined by each microgeometry.

Keywords: Microfluidics, Porous Media, Rheology, Contraction/expansions, Viscoelasticity

1. Introduction

In applications related to the petroleum industry it is a common practice to use additives to impart non-Newtonian properties to aqueous and hydrocarbon systems. These additives are used in water-flood processes for enhanced oil recovery, showing the practical relevance of investigating non-Newtonian fluid flow through porous media (Gaitonde and Middleman, 1966; Marshall and Metzner, 1967). However, in spite of its extensive use over the past fifty years, there is no general approach for a proper description of the flow of complex fluids through porous media (Sochi, 2010).

There is a large variety of experimental systems that have been considered as models of real porous media in flow studies involving complex fluids. Each porous medium is itself unique in its morphology. However, much of the work dealing with the fundamental aspects of porous media involve the use of unconsolidated models (Savins, 1969). For that reason, in this study it was also chosen an unconsolidated packed bed of sand as the porous medium.

Most fluids made from polymer macromolecules exhibit viscoelastic behavior. Viscoelastic solutions commonly exhibit a shear thinning viscosity (of which Boger fluids are an important exception) and fading memory under shear (Macosko, 1994), while their elongational viscosity is both strain and strain rate dependent (Petrie, 2006a,b), and in some cases the Trouton ratio is large. In particular, the strain hardening behavior complicates substantially the analysis of viscoelastic fluid flow through porous medium and so it is not surprising that there is little definitive and quantitative information available on the role of viscoelasticity in the flow through porous media (Chhabra et al., 2001). To provide further insights on this matter, dilute aqueous solutions of polyacrylamide (PAA) were used as model viscoelastic fluids, which is an important polymer used for enhanced oil recovery applications, due to its markedly elastic

behavior and significant strain hardening behavior (Duda et al., 1983).

It is widely accepted that in porous media the converging-diverging flow paths bring out the influence of both the extensional and shear properties of the fluid. Indeed, the shape of the geometry determines the ratio of shearing to extensional contributions. Experimental results suggest that the flow of viscoelastic fluids through packed beds can exhibit a significant increase in the pressure drop with increasing flow rate, above that expected for purely viscous fluids with a similar shear viscosity, but its precise nature is still unclear (Sochi, 2009).
The pore scale within a porous medium is not only difficult to access visually but often characterized by parameters like connectivity, permeability and tortuosity, which are difficult to determine experimentally for inhomogeneous media. As soils like sand have an average particle size of the order of a hundred microns, microchannels containing a series of contractions and expansions arise as simple devices to be used as porous medium analogues. In this work, microfluidic devices with two geometrical arrangements are proposed as simplified 1-D microfluidic analogues of a porous medium. The goal is to assess their applicability to mimic a real porous medium, based on pressure drop measurements for a range of flow rates.

2. Materials and methods

2.1 Characterization of the viscoelastic polymer solutions

In this study, a Newtonian liquid (de-ionized water) and two dilute aqueous solutions of PAA ($Mw = 18\times10^6$ g/mol, Sigma-Aldrich) at weight concentrations of 50 and 125 ppm, hereafter named as PAA50 and PAA125, respectively, were used. According to Sousa et al. (2010) these concentrations are below the critical overlap concentration, c^*. The PAA solutions were prepared by mixing the polymer into the solvent (de-ionized water) at different concentrations, using magnetic stirrers at low angular speeds, in order to avoid mechanical degradation of the polymer molecules. To minimize biological degradation, all solutions were stored in a refrigerator at 4ºC. The density of the fluids was measured at 20 ºC using a calibrated hydrometer: $\rho_{water} = 998.0$ kg/m^3, $\rho_{PAA50} = 998.0$ kg/m^3, $\rho_{PAA125} = 998.2$ kg/m^3.

The rheology of the solutions was characterized under steady shear and uniaxial extensional flow conditions at 20.0 ± 0.1 ºC. A controlled stress rotational rheometer (Physica MCR 301, Anton Paar) was used to determine the flow curves. To measure the shear viscosity over the range of shear rate occurring in porous media (up to 10^4 s^{-1}), a plate-plate geometry was used, with a diameter of $D = 50$ mm and a gap of 100 µm. Three independent runs were carried out to assess the reproducibility of the measurements.

The measurement of the relaxation times of the polymer solutions was performed with a capillary break-up extensional rheometer (Haake CaBER-1, Thermo Scientific) using circular plates with a diameter of $D_p = 6$ mm, an initial separation gap set to $h_i = 3.01$ mm and a final height of $h_f = 12.03$ mm. Subsequently, the stretched liquid filament thins in a process driven by the competing effects of viscoelastic and capillary forces. The time evolution of the mean diameter, $D_{mid}(t)$, curves in the elasto-capillary thinning phase is well described by

$$\frac{D_{mid}(t)}{D_0} = Ce^{(-t/3\lambda)}, \qquad (1)$$

where D_0 is the initial diameter of the filament, C is a fluid dependent constant, t is the time and λ is the relaxation time (Entov and Hinch, 1997). According to Campo-Deaño and Clasen (2010), the longest relaxation times of PAA solutions here considered can be accurately measured with the CaBER technique without any special protocol, given that the zero-shear viscosity of each viscoelastic fluid is sufficiently high (Fig. 1). Nevertheless, at least 20 independent runs were carried out for each fluid to ensure the reproducibility of the

measurements. For quantitative purposes, the relaxation time determined experimentally from the capillary break-up tests by means of Equation 1 (λ_{PAA125} = 129.4 ms and λ_{PAA50} = 54.2 ms) will be used for the calculation of the dimensionless numbers.

a)

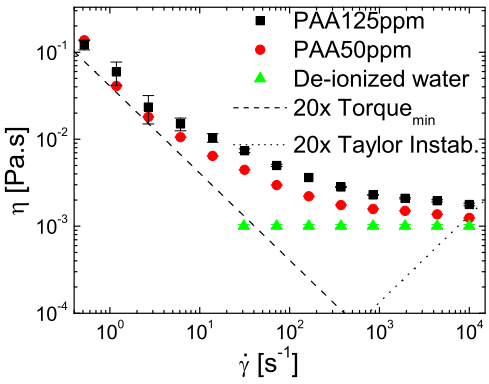

b)

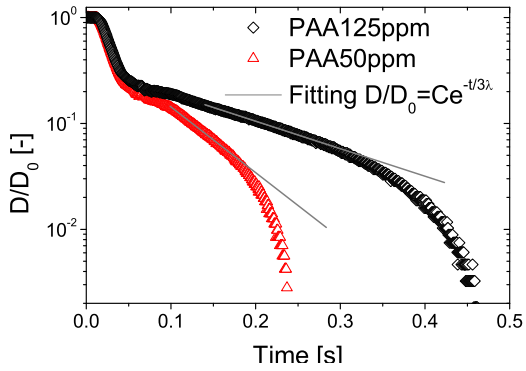

Fig. 1. a) Steady viscosity curve measured for the three working fluids at 20ºC. b) Time evolution of filament thinning for the determination of the longest relaxation time of the two PAA solutions with the capillary break-up rheometer at 20 ºC.

2.2 Porous media analogues

The porous medium is modeled as a bundle of non-uniform microfluidic conduits with a periodic arrangement, each consisting of a continuous series of contractions and expansions in two different arrangements: symmetric and asymmetric (Fig. 2). Both geometries contain 117 repetitive elements. At the widest, narrowest and contraction sections the widths of the microgeometries are W_1, W_2 and W_c, respectively; the lengths of each element are L_1 and L_2; the depth of the channels is uniform and was kept constant for both microdevices studied (H = 100 μm). Table 1 summarizes the dimensions of the microgeometries used in the experiments.

a)

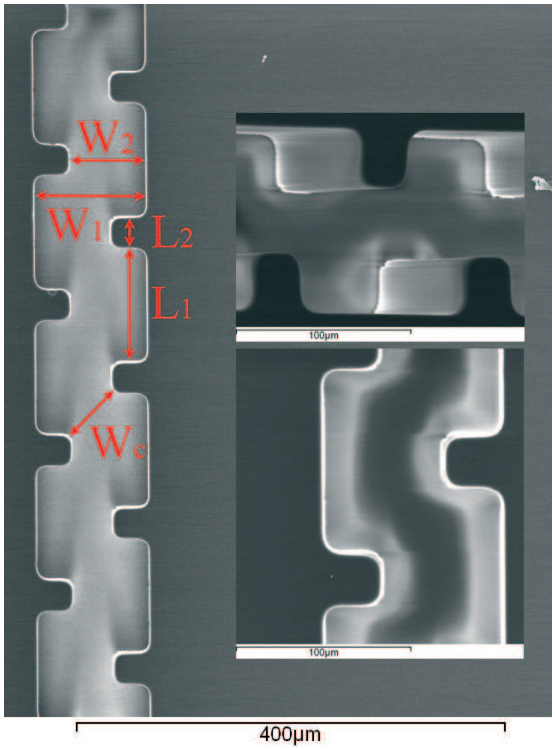

b)

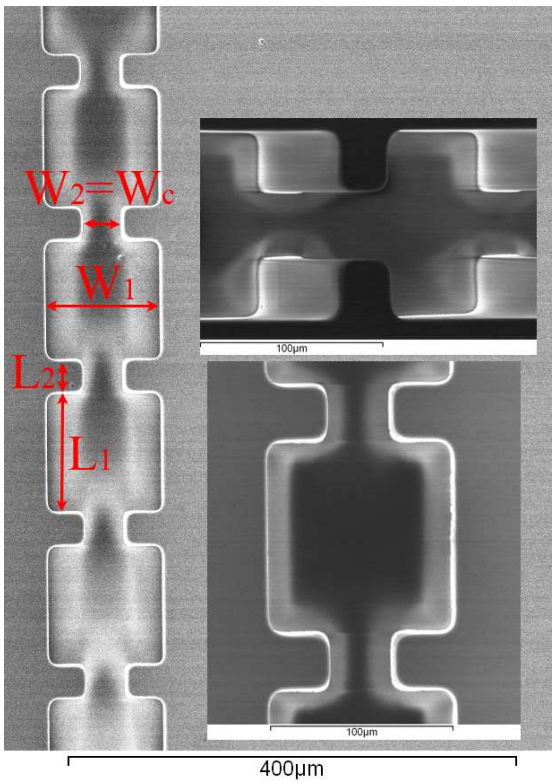

Fig. 2. SEM images of the two microdevices: a) asymmetric configuration; b) symmetric configuration.

Table 1
Dimensions of the microchannels

Dimensions [μm]	Asymmetric	Symmetric
W_1	100	100
W_2	33	33
W_c	46	33
L_1	100	100
L_2	33	33

The flow behavior of Newtonian and non-Newtonian fluids was studied at room temperature (19.5 ± 0.9 ºC) for a wide range of flow rates, which were imposed using a syringe pump (PHD2000, Harvard Apparatus) and Hamilton syringes. The outlet of the microchannels was connected to a reservoir open to the atmosphere where the fluid was collected. The microchannels used in the experiments were fabricated in PDMS using standard soft lithography techniques and SU-8 photo-resist molds.

The pressure drop (ΔP) measurements were carried out by means of calibrated differential pressure sensors (Honeywell 26PC series). The transient response of the pressure sensors was continuously recorded until steady-state was reached.

2.3 Packed bed column

To compare the results of the microchannels with the real porous media (sand bed), the variation of the pressure gradient with flow rate was measured in both systems.

The experimental set-up for the packed bed column (Fig. 3) consists of an acrylic cylindrical tube filled with unconsolidated sand. The internal diameter of the vertical cylinder is 1.95 cm. The vertical alignment is checked with a bubble level before each measurement. The liquid was fed to the column from a pressurized reservoir and thus the inlet pressure could be varied and was measured with a manometer (Wika Instrument Corporation, model 332.50). To avoid the fluidization of the sand bed, the flow inlet was placed at the top of the column and the outlet was located at the bottom part, where the fluid was collected and weighed over the duration of each experiment, in a weighing scale with a resolution of ± 0.01 g. The steady volumetric flow rate was calculated from the measured averaged mass flow rate and the density of the fluid. The pressure drop measurements were carried out between two pressure taps in the column separated by a distance of 14.7 ± 0.1 cm using differential pressure sensors (Honeywell 26PC series) covering values up to ΔP = 200 kPa.

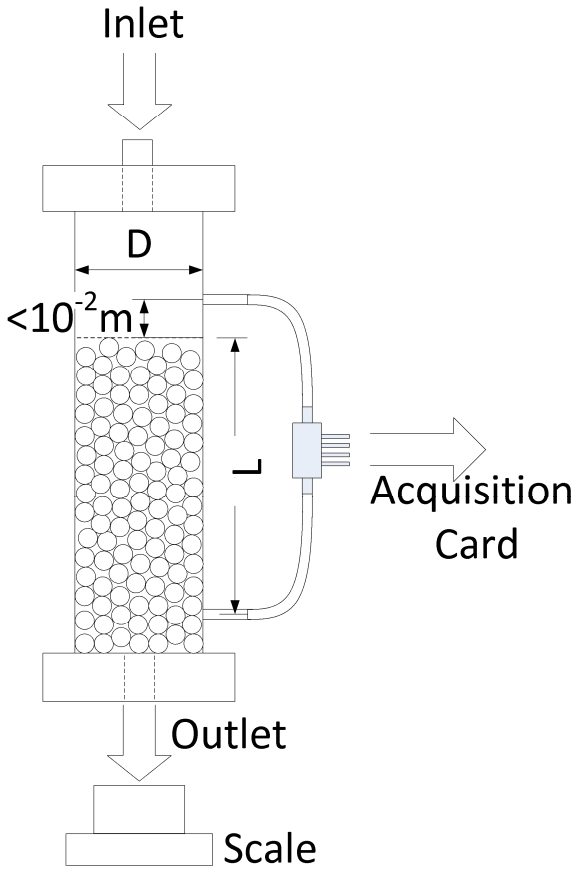

Fig. 3. Experimental set-up for measuring pressure losses of flows through a porous medium. Elements are not to scale

The use of regulating valves in the experimental set-up was intentionally avoided to prevent any unnecessary degradation of the polymer chains beyond that already produced as the fluid flows through the porous medium. The degradation of the polymer chains due to the presence of narrow elements in the set-up could eventually lead to a modification of the rheology of the fluid, and subsequently to a modification in the pressure drop measurements.

The mean Sauter particle size of the sand bed used is x_{32} = 400 μm, with a standard deviation of 90 μm (Fig. 4), as measured by low angle forward scattering (LS™ 230 Laser Diffraction Particle Size Analyzer, Beckman Coulter Inc.). The porosity of the sand beds was also measured, giving $\varepsilon = 0.36 \pm 0.01$.

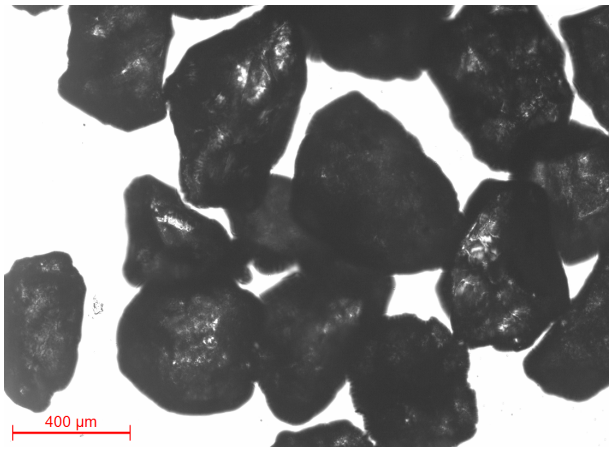

Fig. 4. Image of the sand used in the experiments.

Fig. 5 shows that the measured pressure gradient of de-ionized water in the microfluidic channels and porous medium are similar. In this way it has been confirmed that both microfluidic systems are good analogues of a real porous medium when a Newtonian fluid is used.

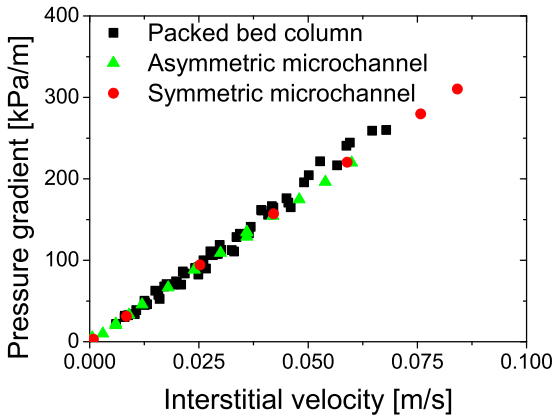

Fig. 5. Pressure gradient as a function of the interstitial velocity for the flow of de-ionized water through the porous medium and through the asymmetric and symmetric microchannels.

3. Results and conclusions

Experiments with aqueous polymer solutions were done in the sand bed with x_{32} = 400 μm.

The pressure gradient in the microchannels was also measured using the PAA solutions to assess the usefulness of the microfluidic devices to mimic the flow of viscoelastic fluids through a porous medium. Fig. 6 shows the pressure gradient curves for both PAA solutions as a function of the Deborah number, which for an isotropic porous medium, can be calculated as

$$De = \lambda \frac{v}{l} \qquad (2)$$

where λ is the longest relaxation time measured in the CaBER for the fresh sample, l is a characteristic length scale (usually taken as the particle mean size) and v is a characteristic velocity (Marshall and Metzner, 1967). The Deborah number represents a ratio of time scales of the material (λ) and of the flow process (l/v), allowing the comparison of the results obtained in the microchannels with those obtained with the sand bed. To calculate the Deborah number from the results obtained in the sand bed, the interstitial velocity ($U_i = U/\varepsilon$) was used as the characteristic velocity, and Sauter's mean diameter (x_{32} = 400 μm) as the characteristic length scale. For the microchannels, the velocity in the contraction sections ($U_{iMC} = Q/W_cH$) was used as the characteristic velocity, while for the characteristic length scale we used the equivalent particle size (dp_{MC} = 420 μm), which was calculated considering the porosity of the selected sand bed (ε = 0.36) to which the microchannels are equivalent to and the corresponding modified permeability of the microchannels ($k'_{MC} = 3.1\text{x}10^{-10}$ m^2). This is determined by the Carman- Kozeny equation (Rhodes, 2008) and the relation between the normal and the modified permeabilities ($k'=k/\varepsilon$).

Fig. 6 shows that, as the *De* is increased, the pressure gradient curve for the asymmetric microchannel is above the curve for the symmetric channel. This enhanced pressure

gradient is due to two simultaneous effects: first, for the same flow rate, the value of the Deborah number is smaller for the asymmetric arrangement

$$De \approx \lambda \frac{U_i}{dp_{MC}} = \lambda \frac{Q}{W_c H dp_{MC}} \qquad (3)$$

which leads to a curve with a larger slope, if we compare identical flow rates in both microfluidic arrangements and without too dissimilar pressure gradients; second, it is currently widely accepted that the underlying mechanism for the onset of purely elastic flow instabilities is related to streamline curvature, and the development of large hoop stresses, which generates tension along fluid streamlines leading to flow destabilization (Larson et al., 1990; Pakdel and McKinley, 1996; McKinley et al., 1996). According to this argument, and since the flow streamlines in the asymmetric configuration have more curvature than in the symmetric channel, it is expected that there would be an extra contribution to the pressure gradient in the former. Since the onset of elastic instabilities occurs at lower *De* in the asymmetric than in the symmetric configuration, this is an indirect evidence of the higher $\Delta P/L$ *vs. De* slope observed for the asymmetric microchannel.
This analysis is further corroborated in the insets of Fig. 4 for low flow rates, where both microchannels and the real porous medium essentially exhibit the same Newtonian-limit behavior. This is a consequence of both the absence or the small magnitude of elastic effects taking place at low flow rates (or *De*). Moreover, it is also worth noting that the curve obtained for the real porous medium lies between those obtained for the microchannels. In real porous media, it can be clearly observed a critical value of the Deborah number (De_{cr}) above which the pressure gradient rises significantly due to elastic effects that also grow with the flow rate. For the PAA solutions here considered, this critical value is $De_{cr} \approx 1.6$, as it is clear from Fig. 4, where a sudden change of slope is seen to take place.

The real porous medium is in reality a random mixture of the two arrangements of particles simulated with the microchannels, which can be considered as limiting ideal configurations. The results show that the symmetric microchannel describes better the viscoelastic fluid flow through a porous medium at low *De* (between the end of the Newtonian-like behavior and the critical flow rate) than the asymmetric configuration. However, extrapolating the results to higher values of *De*, beyond those achieved here, it seems that under such conditions, the asymmetric configuration would be a more suitable description of the real porous medium, especially for the highest polymer concentrations.

a)

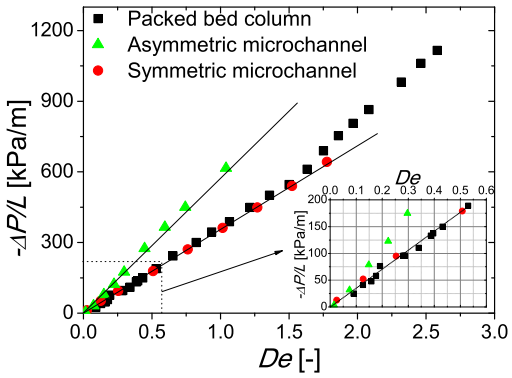

b)

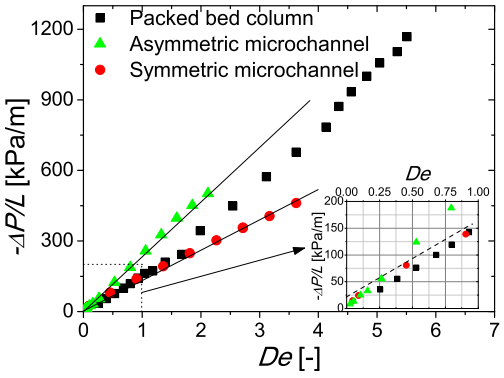

Fig. 6. Pressure gradient as a function of the Deborah number for the flow of the viscoelastic fluids through the porous medium and through the asymmetric and symmetric microchannels: a) PAA50; b) PAA125 fluids.

Acknowledgements
Authors acknowledge financial support from Fundação para a Ciência e a Tecnologia (FCT), COMPETE and FEDER through projects PTDC/ EQU-FTT/ 71800/ 2006, PTDC/EQU-FTT/ 70727/ 2006, PTDC/ EME-MFE/ 99109/ 2008 and REEQ/ 262/ EME/ 2005. The technical support of L.C. Matos is also acknowledged. F.J. Galindo-Rosales would like to acknowledge FCT for financial support (scholarship SFRH/BPD/69663/ 2010).

References
Campo-Deaño, L., Clasen, C., 2010. The slow retraction method (SRM) for the determination of ultra-short relaxation times in capillary breakup extensional rheometry experiments. Journal of Non-Newtonian Fluid Mechanics 165, 1688-1699.

Chhabra, R.P., Comiti, J., Machac, I., 2001. Flow of non-Newtonian fluids in fixed and fluidised beds. Chem. Eng. Science 56, 1-27.

Duda, J.L., Hong, S.A., Klaus, E.E., 1983. Flow of polymer solutions in porous media: Inadequacy of the capillary model. Industrial and Engineering Chemistry Fundamentals 22, 299-305.

Entov, V.M., Hinch, E.J., 1997. Effect of a spectrum of relaxation times on the capillary thinning of a filament of elastic liquid. Journal of Colloid and Interface Science 72(1), 31-51.

Gaitonde, N.Y., and Middleman, S., 1966. Flow of viscoelastic fluids through porous media. Industrial and Engineering Chemical Fundamentals 6(1), 145-147.

Larson, R.G., Shaqfeh, E.S.G., Muller, S.J., 1990. A purely elastic instability in Taylor-Couette ow. Journal of Non-Newtonian Fluid Mechanics 218, 573-600.

Macosko, C.W., 1994. Rheology: Principles, measurements, and applications. Wiley-VCH, Inc., New York.

Marshall, R.J., and Metzner, A.B., 1967. Flow of viscoelastic fluids through porous media. Industrial and Engineering Chemical Fundamentals 6(3), 393-400.

McKinley, G.H., Pakdel, P., Oztekin, A., 1996. Rheological and geometric scaling of purely elastic ow instabilities. Journal of Non-Newtonian Fluid Mechanics 67, 19-47.

Pakdel, P., McKinley, G.H., 1996. Elastic instability and curved streamlines. Physical Review Letters 77, 2459-462.

Petrie, C.J.S., 2006a. Extensional viscosity: A critical discussion. Journal of Non-Newtonian Fluid Mechanics 137, 15-23.

Petrie, C.J.S., 2006b. One hundred years of extensional flow. Journal of Non-Newtonian Fluid Mechanics 137, 1-14.

Rodd, L.E., Scott, T.P., Boger, D.V., Cooper-White, J.J., McKinley, G.H., 2005. The inertio-elastic planar entry ow of low-viscosity elastic fluids in microfabricated geometries. Journal of non-Newtonian Fluid Mechanics 129, 1-22.

Rhodes, M. 2008. Introduction to particle technology. 2nd Edition. John Wiley & Sons, Ltd. England.

Savins, J.G., 1969. Non-Newtonian ow through porous media. Industrial and Engineering Chemistry 61(10), 18-47.

Sochi, T., 2009. Pore-scale modeling of viscoelastic flow in porous media using a Bautista-Manero fluid. International Journal of Heat and Fluid Flow 30, 1202-1217.

Sochi, T., 2010. Flow of non-Newtonian fluids in porous media. Journal of Polymer Science: Part B: Polymer Physics 48, 2437-2467.

Sousa, P.C., Pinho, F.T., Oliveira, M.S.N., Alves, M.A., 2010. Efficient microfluidic rectifiers for viscoelastic fluid flow. Journal of Non-Newtonian Fluid Mechanics 165, 652-671.